ELSEVIER

Catalysis Today 76 (2002) 177–188

CATALYSIS TODAY

www.elsevier.com/locate/cattod

Effects of radiation absorption and catalyst concentration on the photocatalytic degradation of pollutants

D. Curcó, J. Giménez*, A. Addardak, S. Cervera-March, S. Esplugas

Departamento de Ingeniería Química, Facultad de Química, Universidad de Barcelona, C/Martí i Franquès 1, 08028 Barcelona, Spain

Abstract

This study is dealing with the reaction rate dependence on catalyst concentration and light absorption in photocatalytic processes. Models relating the reaction rate to the absorbed radiation by the catalyst (titania in suspension) are proposed. To apply these models, the system is divided into layers and each layer is divided into cells, assuming that there is only one particle (agglomerate) of catalyst in each cell. The extensive reaction rate can be calculated as the sum of the reaction rate in each cell, being this proportional to the light absorbed by each particle. Two different models are proposed for light propagation through the reaction medium (exponential and probabilistic model). The extinction coefficients have been estimated by using transmittance measurements related to sedimentation rates changing according to catalyst concentration and pH. The integration of these models, taking into account the expression of the reaction rate, allows to obtain equations that can explain the trends observed in the photocatalytic treatment of Cr(VI) and phenol, by using TiO_2 (Degussa-P25) in suspension.

Keywords: Photocatalysis; Radiation models; Reactor modeling; Pollutants treatment; Kinetic models

1. Introduction

An interesting problem related to the photocatalytic processes is the one concerning the relationship between catalyst concentration and reaction rate, by considering the radiation absorption at the same time.

Kinetic studies on photocatalysis normally show that the reaction rate increases with catalyst concentration. However, the kinetic constant reaches a maximum value for catalyst concentrations between 0.2 and 1 g/l, depending on the compound and the photoreactor used, and after that, it remains unchanged or decreases slowly when catalyst concentration is increased [1–4]. Several reasons can explain this behavior, for instance, the influence of radiation field.

Different models have been proposed in the literature where the problem has been studied from various points of view. Several relationships have also been obtained allowing to estimate the radiation absorbed by the catalyst [5–8]. Some authors, being the Cassano's group the most representative, focus their efforts on the modeling of the radiation field in a double aspect: radiation entering the system and distribution of this radiation inside the system [9–18]. These models have the starting point in the radiation models for homogeneous systems and the heterogeneity is considered by introducing scattering or by assuming an effective absorption coefficient. Thus, from the integration of microscopic radiation balances, models describing the radiation field are obtained. Other models [19–21] overcome the need of integrating the

* Corresponding author. Tel.: +34-93-402-1293; fax: +34-93-402-1291.
E-mail address: gimenez@angel.qui.ub.es (J. Giménez).

0920-5861/02/$ – see front matter
PII: S0920-5861(02)00217-1

Nomenclature

c_p	catalyst concentration ($g\,cm^{-3}$)
d	distance traveled by a photon (cm)
D	agglomerate diameter (cm)
$f(c)$	function of the reactants concentration
f_i	probability that a photon impacts against i agglomerates
f'_1	probability that a photon impacts against i agglomerates and continues
$F(i)$	radiation absorbed in the layer i ($eins\,s^{-1}$)
$F(i, j)$	radiation absorbed in the cell (i,j) ($eins\,s^{-1}$)
F_0	photonic flux entering a reactor ($eins\,s^{-1}$)
g	specific gravity ($9.8\,m/s^2$)
h	length of a cell containing one agglomerate (cm)
i	natural number describing a layer i
j	natural number describing a cell j in each layer
k	global kinetic constant
k_a	intrinsic kinetic constant, independent on the agglomerates size, catalyst concentration and radiation entering a reactor
k_b	coefficient affecting the β parameter
k_{max}	maximum value of kinetic constant in the experimental range considered
L_T	length of the spectrophotometer detector (m)
n_c	inverse of h
n_p	number of agglomerates or cells in a layer
n_s	coefficient affecting the parameter β
P_x	probability of a photon to impact against an agglomerate through a length h
P'_x	probability of a photon to impact against an agglomerate through a length h if photons would behave as corpuscles
Q_a	absorption coefficient
Q_{bs}	backward scattering coefficient
Q_e	extinction coefficient
Q_{fs}	forward scattering coefficient
$R(i, j)$	extensive reaction rate in a cell ($mol\,s^{-1}$)
R	extensive reaction rate in the system ($mol\,s^{-1}$)
S_f	illuminated surface of the reactor (cm^2)
T	transmittance in tant per one
T_f	transmittance when the sedimentation front reaches the final of the spectrophotometer detector
T_i	transmittance when the sedimentation front reaches the top of the spectrophotometer detector
v_s	sedimentation rate (m/s)
V	reaction volume (cm^3)

Greek symbols

β	exponent of the photonic flux absorbed by an agglomerate, depending on position
μ_w	viscosity of water ($kg\,m^{-1}\,s^{-1}$)
ρ_s	catalyst density ($g\,cm^{-3}$)
ρ_w	density of water
σ_a	absorption coefficient for titania suspension ($cm^2\,g^{-1}$)
σ_{bs}	backward scattering coefficient ($cm^2\,g^{-1}$)
σ_e	extinction coefficient of a suspension ($cm^2\,g^{-1}$)
σ_{ef}	experimental extinction coefficient for each particular suspension of TiO_2 ($cm^2\,g^{-1}$)
σ_{fs}	forward scattering coefficient ($cm^2\,g^{-1}$)

radiation balances by using the Monte Carlo technique.

The objective of this paper is to establish useful models to relate the reaction rate to the amount and distribution of radiation inside a photocatalytic system, by connecting all that to the catalyst concentration. The models are based on experimental parameters that can be estimated in each particular case driving to a more specific description of the process studied. For this reason, these models represent also a general form useful for any photocatalytic process. In addition, the final equations are not so difficult to solve.

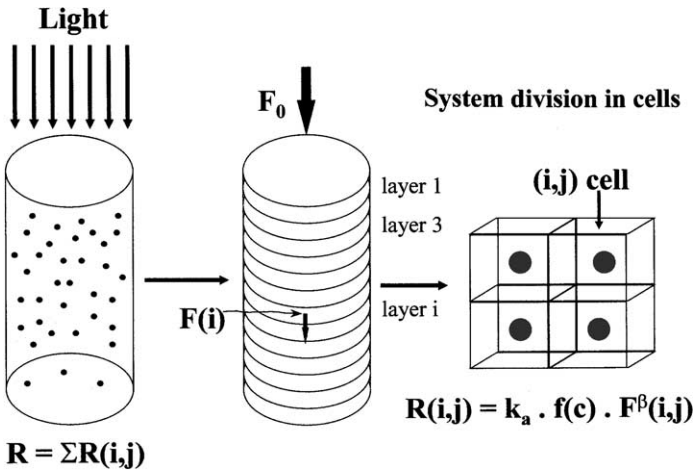

Fig. 1. System division in cells.

The proposed models are based on the assumption that the reactor is divided into layers, and each layer is divided into cells with the same volume. Thus, the extensive reaction rate is the sum of the reaction rates in the cells (see Fig. 1). It is also assumed that there is only one particle (agglomerate) in each cell, and it is differently illuminated depending on its position. In this way, the reaction rate $R(i, j)$ in each cell can be expressed as

$$R(i, j) = k_a f(c) F^{\beta}(i, j) \quad (1)$$

where k_a is the kinetic constant, $f(c)$ is a function of reactants and products concentration, $F(i, j)$ the absorbed radiation in each cell, "i" being the number of the layer, and "j" is the position of the cell inside the layer. β is a coefficient between 0 and 1 [4,22–29], which depends on the extinction coefficient (σ_e), catalyst concentration (c_p), and the distance from the considered agglomerate to the surface of solution.

The total extensive reaction rate (R) will be the sum of the contributions of all cells:

$$R = \sum_i \sum_j R(i, j) \quad (2)$$

where i represents the position of each layer in the reactor and j represents the position of each cell in each layer.

The next question is how to estimate the absorbed radiation in each cell. This can be solved by assuming that radiation propagates following an exponential or a probabilistic model. In the exponential model, the amount of radiation decreases exponentially with the distance, and catalyst concentration, following the Lambert–Beer law. In the probabilistic model, the amount of radiation decreases following a potential model. The absorbed radiation is expressed as a function of the entering radiation and the probability that a photon impacts against an agglomerate.

Both models will be discussed and solved. Some optical parameters, needed to solve models, were determined by using different experimental methods. The results of previously reported experiments [23,24,30–32] on the photocatalytic treatment of phenol and Cr(VI) are used to test the proposed models.

2. Experimental

To apply the models, it is necessary to know some optical parameters, being among them the extinction coefficients. These can be estimated from transmittance measurements. For this, different spectrophotometers have been used. Some measurements of the transmittances of suspensions have been carried out with a Lambda UV20 spectrophotometer from Perkin-Elmer. This spectrophotometer has a wide cuvette receptacle (see Fig. 2) in such a way that a

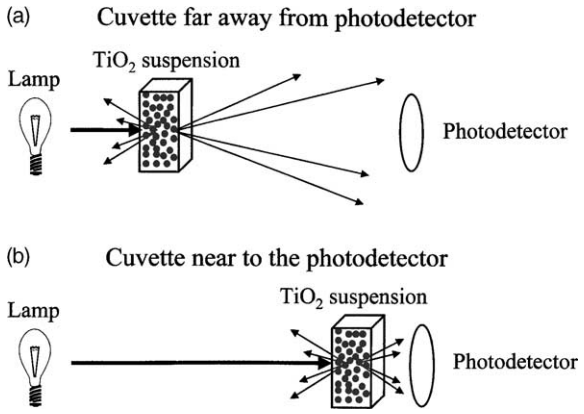

Fig. 2. Transmittance measurements in the spectrophotometer varying the distance from the cuvette to the photodetector.

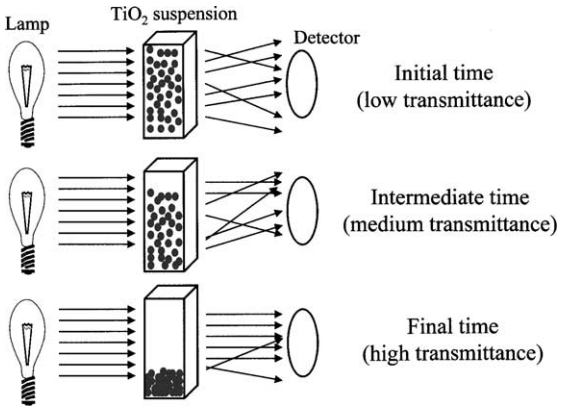

Fig. 3. Photosedimentation measurements. Variation of transmittance during time for suspensions of titania.

quartz cuvette (1 cm width) can be placed close to the photodetector or quite far away (10 cm). This availability has been used to study the forward scattered radiation (σ_{fs}). The suspensions were prepared with TiO_2 Degussa P-25, adding the corresponding amount of H_2SO_4 (RG) to achieve the desired pH (between 1 and 4). The titania concentration was varied between 0 and 2 g/l.

A Shimadzu Scanning UV-Vis 2101 PC spectrophotometer has also been used, with the double purpose of measuring the total transmitted light and the reflectance of the suspensions. Combinations of the measurements with these devices allowed us to estimate the different contributions, absorption (σ_a) and scattering ($\sigma_{fs} + \sigma_{bs}$), to the total extinction of light through the suspensions [7]. The measurements have been carried out in the corresponding wavelength range (300–400 nm).

As shown in Fig. 3, the spectrophotometer has also been used to study the variation of the transmittance of TiO_2 suspensions during time. Of course, transmittance depends on catalyst concentration and pH. As an example, the obtained transmittances at pH 3, for different catalyst concentrations, are shown in Fig. 4.

The relationship between transmittance and sedimentation rate is shown in Fig. 5, in a qualitative manner. At the initial time (t_0) the suspension is homogeneously distributed in the cuvette. Then, sedimentation starts and different zones appear in the cuvette with different agglomerates distribution. At time t_i, the sedimentation front reaches the top of the spectrophotometer detector and transmittance increases more quickly. Between time t_i and time t_f (transmittance T_f), the detector can "see" the sedimentation front and transmittance continues increasing. Note that the time between t_i and t_f is the time needed for the sedimentation front to travel the length (L_T) of the detector. From t_f to the final time, transmittance remains practically unchanged.

The variation of the transmittance can be related to the rate of sedimentation (v_s) by Eq. (3):

$$v_s = \frac{T_f - T_i}{L_T} \frac{dT}{dt} \tag{3}$$

where dT/dt can be estimated from the slope of the curves of transmittance v_s time.

By using momentum balance, the rate of sedimentation can be related to the diameter (D) of agglomerates. The equation relating them, by assuming an average size and spherical shapes, is the following:

$$D = \sqrt{\frac{18 v_s \mu_w}{g(\rho_{TiO_2} - \rho_w)}} \tag{4}$$

μ_w being the viscosity of water, ρ_w the density of water, ρ_s the density of catalyst (titania in this case), and g the specific gravity.

Thus, by using Eq. (4), the agglomerate diameters can be estimated. This technique allows to reproduce the experimental conditions used in the kinetic experiments, and for this reason, the agglomerate diameters obtained are closer to the values occurring in experiments for the photocatalytic destruction of pollutants.

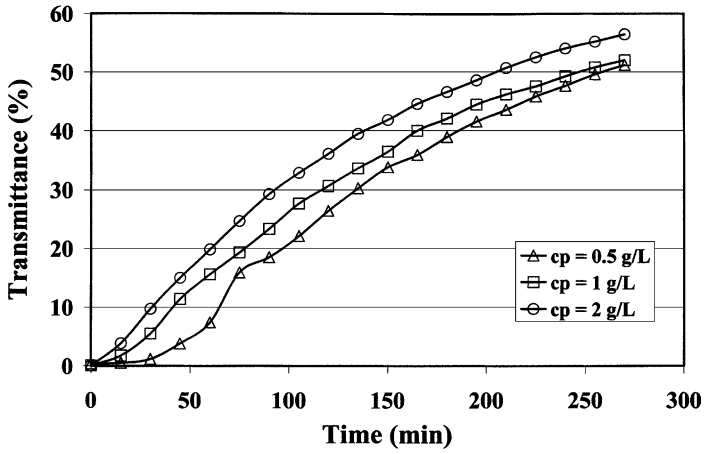

Fig. 4. Variation of transmittance with TiO_2 concentration at pH 3.

As reaction models, the photocatalytic treatments of Cr(VI) and phenol have been chosen, as examples of inorganic and organic pollutants and reduction and oxidation treatments. The kinetic experiments and the results obtained in the treatment of these two pollutants have been widely discussed in previous papers [23,24,30–32]. The photocatalyst used was TiO_2 Degussa P-25 its concentration was varied between 0 and 2 g/l. The experiments were carried out inside a Solarbox (CO.FO.ME.GRA) with a 1500 W Xe lamp. A flat photoreactor was used with an upper area of 23 cm^2 and a volume of c.a. 100 ml. The reactor is located at the bottom (center) of the Solarbox. The lateral walls of the reactor were covered in all cases so that radiation enters the photoreactor only through its upper surface. Actinometric measurements have shown that radiation was entering perpendicular to the reactor. In addition, the design of Solarbox satisfies this assumption because reflectors are placed at the top of the Solarbox (back of the lamp) and in the lateral walls,

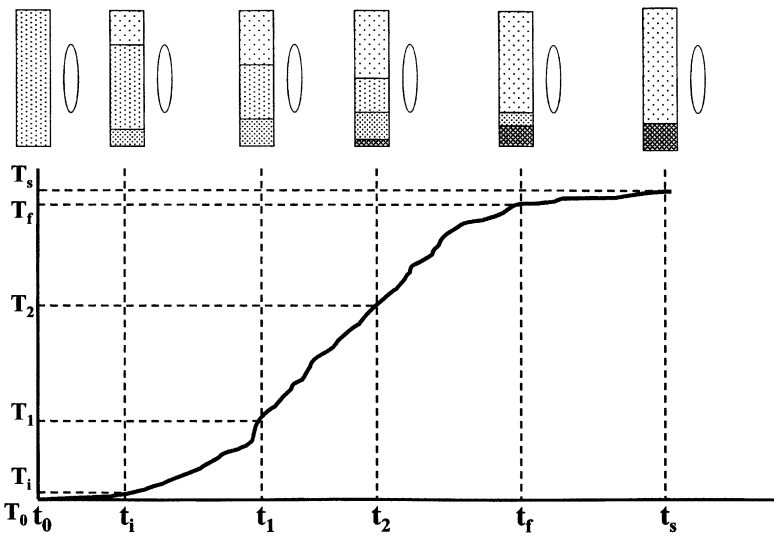

Fig. 5. Evolution of sedimentation and transmittance during time.

driving rays perpendicular to the bottom of Solarbox. The reactor was vigorously stirred by magnetic stirring and perfect mixing flow was assumed. The evolution of phenol concentration with time was followed with a Hewlett-Packard 5890 Series II Gas Chromatograph, as already explained in previous papers [23,33]. The chromium was analyzed by UV spectrophotometry by measuring the absorbance variation with chromium concentration [30].

3. Results and discussion

3.1. Results obtained in the treatment of Cr(VI) and phenol

The experimental series consisted of evaluating the different reaction rates and kinetic constants at several catalyst concentrations. As commented before, the experimental conditions and the results obtained, including the absolute values for the kinetic constants, were previously reported [23,24,30–32]. Fig. 6 summarizes the results obtained. In order to compare Cr(VI) and phenol, it is represented the quotient between the kinetic constant at each catalyst concentration and the maximum value for the kinetic constant obtained for each pollutant.

3.2. Cells model

The reaction rate in each cell ($R(i, j)$) is related to the radiation absorbed ($F(i, j)$) in this cell (Eq. (1)),

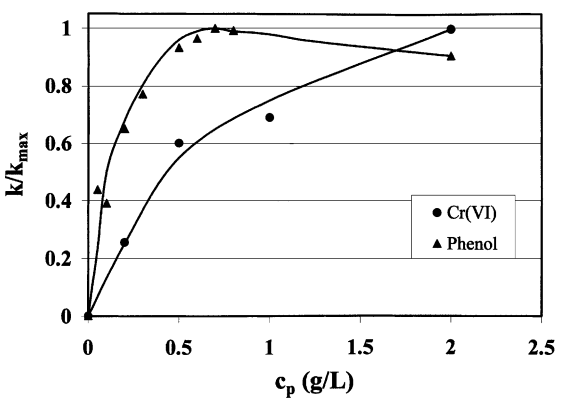

Fig. 6. Results obtained in the photocatalytic treatment of phenol and Cr(VI) by different concentrations of titania.

and ($F(i, j)$) depends on the geometrical and physical characteristics of the system. We consider a flat reactor with an infinite depth and illuminated from an infinitely far light source in such a way that the incoming rays are perpendicular to the surface. The reactor is divided into cells of length h [8,20,21] and each cell contains only one catalyst agglomerate (see Fig. 1). Assuming that all the agglomerates are spherical and have the same size, the length of the cell (h) is given by

$$h = \left(\frac{\pi\rho_s}{6c_p}\right)^{1/3} D \tag{5}$$

ρ_s being the catalyst density, c_p the catalyst concentration, and D is the diameter of the agglomerates.

If the illuminated reactor surface has an area S_f, the number (n_p) of agglomerates in a layer will be

$$n_p = \frac{S_f}{h^2} = S_f \left(\frac{6}{\pi\rho_s}\right)^{2/3} \frac{c_p^{2/3}}{D^2} \tag{6}$$

Given the symmetry of the system, $F(i, j)$ can be expressed as

$$F(i, j) = \frac{F(i)}{n_p} \tag{7}$$

$F(i)$ being the absorbed photonic flux in the layer "i" (see Fig. 1).

According to Eq. (2), the total extensive reaction rate (R) has to be equal to the sum of all the extensive reaction rates ($R(i, j)$) corresponding to each cell (Eq. (1)). Thus, by using Eqs. (1), (2), (5)–(7):

$$R = k_a f(c) n_p \sum_{i=1}^{\infty} \frac{F^\beta(i)}{n_p^\beta} = k_a f(c) n_p^{1-\beta} \sum_{i=1}^{\infty} F^\beta(i) \tag{8}$$

The sum is extended to infinite in order to simplify the expression. This assumption does not affect later calculations because the deepest layers have not any weight in the value of the calculated R (they are practically dark layers). Note the difference between Eq. (8) and the expression normally used (Eq. (9)) for the extensive reaction rate when only the time influence is considered

$$R = kVf(c) \tag{9}$$

If Eqs. (8) and (9) are compared (see Eq. (10)), it appears that the global kinetic constant (k), represented

in Fig. 6, includes terms that can vary with time, agglomerates position, radiation used, etc. On the contrary, k_a does not depend on these parameters and can be used in other experimental devices or conditions different from the tested ones, which is not true for k.

$$k = k_a \frac{n_p^{1-\beta}}{V} \sum_{i=1}^{\infty} F^{\beta}(i) \tag{10}$$

The dependence of the summatory of $F^{\beta}(i)$ on the distance to the illuminated surface and on the catalyst concentration is given by the considered radiation model. As commented in Section 1, two different models for radiation propagation have been considered: the exponential and the probabilistic model.

3.3. Exponential model

In the exponential model, the function relating the absorbed radiation to the entering radiation (F_0) can be expressed in a general form by

$$F = F_0 \exp(-\sigma_e c_p d) \tag{11}$$

where σ_e is the extinction coefficient, and d is the distance followed by a photon from the reactor entrance to the position of the considered agglomerate.

Along a layer "i" the absorbed radiation $F(i)$ (see Fig. 7) is given by

Absorbed radiation in i = radiation entering from $(i-1)$-radiation coming out from i

$$\begin{aligned} F(i) &= F_0 \exp[-\sigma_e c_p h(i-1)] - F_0 \exp[-\sigma_e c_p hi] \\ &= F_0 \exp[-\sigma_e c_p hi](\exp[\sigma_e c_p h] - 1) \end{aligned} \tag{12}$$

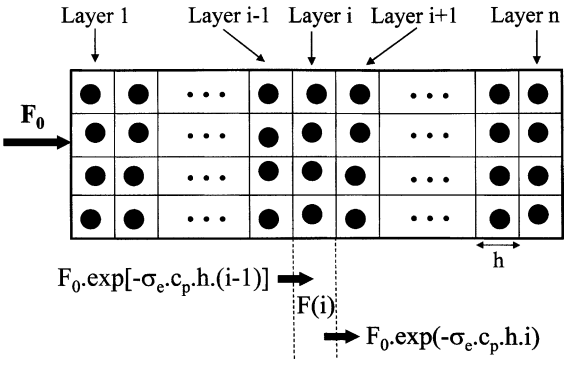

Fig. 7. Evaluation of the radiation absorbed in each layer by using the exponential model.

where F_0 is the photonic flux entering the system (eins s^{-1}). Substituting Eq. (12) into Eq. (8), we have

$$\begin{aligned} R &= k_a f(c) n_p^{1-\beta} F_0^{\beta} (\exp[\sigma_e c_p h] - 1)^{\beta} \\ &\quad \times \sum_{i=1}^{\infty} \exp[-\sigma_e \beta c_p hi] \end{aligned} \tag{13}$$

Taking into account the mathematical relationship

$$\sum_{i=1}^{\infty} \exp[-ix] = \frac{1}{\exp[x] - 1} \tag{14}$$

and, by considering Eq. (5), Eq. (13) becomes

$$\begin{aligned} R &= k_a F_0^{\beta} S_f^{1-\beta} f(c) \left(\frac{6}{\pi \rho_s}\right)^{2(1-\beta)/3} \frac{c_p^{2(1-\beta)/3}}{D^{2(1-\beta)}} \\ &\quad \times \frac{(\exp(\sigma_e (6/\pi\rho_s)^{1/3} c_p^{2/3} D) - 1)^{\beta}}{\exp(\sigma_e \beta (6/\pi\rho_s)^{1/3} c_p^{2/3} D) - 1} \end{aligned} \tag{15}$$

Up to now, the diameter of the agglomerates (D) has been considered constant. However, by photosedimentation measurements in the spectrophotometer (as explained in Section 2, see Figs. 3–5 and Eq. (4)), it can be demonstrated that the size of agglomerates changes with concentration. From previous experimental measurements [30], the following relationship has been obtained for pH 1–4

$$D = 550 \ln(c_p) + 7160 \quad (D, \text{ nm}; c_p, \text{ g cm}^{-3}) \tag{16}$$

Another hypothesis to consider is that parameter β does not vary with the depth of the considered layer. It seems logical to think that parameter β (which is lower as more illuminated is the catalyst) will be higher as deeper is the considered layer, and it can also vary depending on the photodegradated substance [34,35]. Thus, it can be considered that parameter β should vary along the system in such a way that in the more illuminated layers its value is 1/2 (the incoming radiation inside the photoreactor is around 1 Sun) while in the darkest zones its value is 1. In this way, the variation of β through the layers could follow a trend such as

$$\beta = \frac{1 + k_b \sigma_e c_p^{n_s} hi}{2 + k_b \sigma_e c_p^{n_s} hi} \tag{17}$$

This function allows us to consider the variation of β with the illumination to explain the dependence

of the kinetic reaction rate on the agglomerates concentration. k_b and n_s are parameters depending on the particular system studied and they can be varied for fitting the models. Summarizing, Eqs. (16) and (17) have to be introduced into Eq. (15) in order to determine the dependence of reaction rate on the catalyst concentration and radiation. However, to apply Eq. (15), we need to know the extinction coefficient (σ_e). This coefficient can be expressed by Eq. (18):

$$\sigma_e = \sigma_a + \sigma_{fs} + \sigma_{bs} \quad (18)$$

This equation reflects the contribution of each phenomenon to the extinction coefficient. Thus, σ_a is the absorption coefficient related to the radiation absorbed by the catalyst, and σ_{fs} and σ_{bs} represent the contribution of forward and backward scattering, respectively. When a 1 cm width cuvette is placed in the spectrophotometer and far enough from the photodetector (see Fig. 2), the transmittance (T) measured by the detector can be expressed as

$$T = \exp(-\sigma_{ef} c_p d) \quad (19)$$

where c_p is the catalyst concentration, d the distance followed by each photon (width cuvette), and σ_{ef} is the extinction coefficient of the particular suspension of TiO_2 used.

Knowing c_p, d, and the experimental values of T, it is possible to calculate σ_{ef}. This extinction coefficient is related to the part of the radiation coming from the lamp that does not reach the photodetector. In this case, it is the radiation absorbed by titania agglomerates, or backward or forward scattered (see Fig. 2). Thus, σ_{ef} can be expressed as

$$\sigma_{ef} = \sigma_a + \sigma_{fs} + \sigma_{bs} \quad (20)$$

As an example, Fig. 8 illustrates the variation of the absorption coefficient and forward scattering coefficient with the wavelength. In the particular case studied, the backward scattering coefficient was much more lower than the others and it can be neglected.

In the case studied, Eqs. (18) and (20) are the same. This means that measurements by spectrophotometer give directly the value of σ_e. This value is used in Eq. (15), together with β and D values previously calculated (Eqs. (16) and (17)), to estimate the real kinetic constant k_a, knowing the extensive reaction rate (R) obtained from experimental data. Finally, to allow

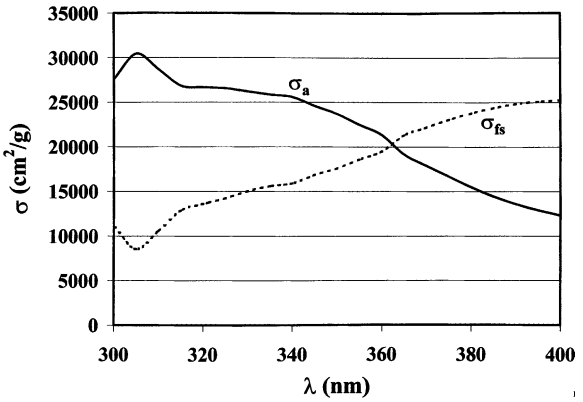

Fig. 8. Variation of extinction coefficients with wavelength.

comparison with the experimental values, by using Eq. (10) and these values of k_a, the corresponding values of k were obtained.

Fig. 9 depicts the obtained results. For comparison between pollutants and models, the quotient between k and maximum value (k_{max}) is represented in the range of catalyst concentrations tested for each pollutant. By comparison of Figs. 6 and 9, it can be seen that the proposed model (Eq. (15)) follows the trend observed for the experimental data.

3.4. Probabilistic model

The exponential model, explained until so far, is in fact an extrapolation from homogeneous media to heterogeneous systems. This point forward considers

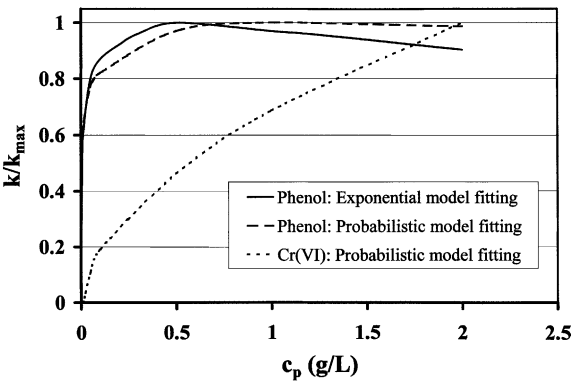

Fig. 9. Results obtained by using the cells model with the exponential and probabilistic models. These curves correspond to the experimental results depicted in Fig. 6.

the opposite approximation for the radiation model. That is, in a particulate system things can occur similarly as in a macroscopic system (high particles volume). Again, the system is divided into cells, each one containing one agglomerate (Fig. 1).

The probability (P'_x) of a ray to impact against an agglomerate, when it travels through the cell, is given by the quotient between the projected area of the agglomerate and the surface of the cell, that is to say

$$P'_x = \frac{\pi D^2}{4h^2} \tag{21}$$

For systems with relatively small agglomerates, Eq. (21) (only valid for macroscopic particles) can be modified by using an extinction coefficient Q_e [36] that takes into account the interference phenomena occurring between particles and light waves. Then, an effective impact probability (P_x) is defined as

$$P_x = \frac{\pi D^2}{4h^2} Q_e = \frac{\pi}{4} \left(\frac{6}{\pi \rho_s}\right)^{2/3} c_p^{2/3} Q_e \tag{22}$$

being the product $\pi D^2 Q_e/4$ a kind of effective cross section area [37].

The amount of radiation absorbed in a layer "i" can be expressed by Eq. (23) (see Fig. 10):

$$F(i) = F_0 P_x (1 - P_x)^{i-1} \left(\frac{Q_a}{Q_e}\right) \tag{23}$$

The quotient Q_a/Q_e introduces the percentage of radiation reaching layer i that is absorbed by catalyst agglomerates, Q_a being the coefficient of absorption.

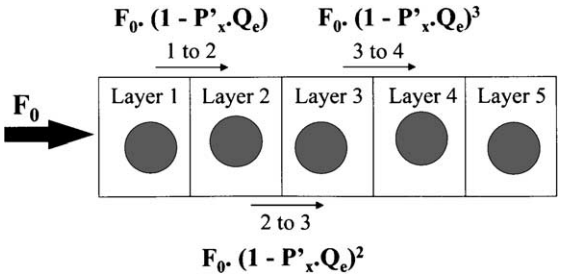

Fig. 10. Radiation arriving to each layer by using probabilistic model.

Substituting Eq. (23) in Eq. (8) we have

$$R = k_a f(c) n_p \sum_{i=1}^{\infty} \frac{F^\beta(i)}{n_p^\beta}$$
$$= k_a f(c) n_p^{1-\beta} F_0^\beta P_x^\beta \left(\frac{Q_a}{Q_e}\right)^\beta \sum_{i=1}^{\infty} (1 - P_x)^{\beta(i-1)} \tag{24}$$

In order to simplify Eq. (24), it can be considered that

$$x \sum_{i=1}^{\infty} (1 - x)^{i-1} = 1 \tag{25}$$

This mathematical relationship is true when $0 < x < 1$. This is the case, because $0 < P_x < 1$. Thus, Eq. (24) becomes

$$R = k_a f(c) F_0^\beta n_p^{1-\beta} \frac{P_x^\beta}{1 - (1 - P_x)^\beta} \left(\frac{Q_a}{Q_e}\right)^\beta \tag{26}$$

In a similar way to the exponential model, taking into account Eqs. (6) and (22), Eq. (26) becomes

$$R = k_a f(c) F_0^\beta S_f^{1-\beta} \left(\frac{6}{\pi \rho_s}\right)^{2(1-\beta)/3} \frac{c_p^{2(1-\beta)/3}}{D^{2(1-\beta)}}$$
$$\times \frac{(\pi/4)^\beta (6/\pi\rho_s)^{2\beta/3} c_p^{2\beta/3} Q_a^\beta}{1 - (1 - [(\pi/4)(6/\pi\rho_s)^{2/3} c_p^{2/3} Q_e])^\beta} \tag{27}$$

Q_e can be estimated from spectrophotometric measurements by using Eq. (28):

$$T = (1 - P'_x Q_e)^{n_c} \tag{28}$$

where T is the experimental transmittance measured by the detector, for each wavelength and each catalyst concentration, and n_c is defined as $1/h$.

For the calculation of R (Eq. (27)), we also need to know the value of Q_a, that can be evaluated as in the case of the exponential model. Thus, Q_e can be expressed by

$$Q_e = Q_a + Q_{fs} + Q_{bs} \tag{29}$$

where Q_{bs} and Q_{fs} represent the coefficients for backward and forward scattering, respectively. Q_{bs} can be assimilated to the reflectivity. Thus, measurements of the reflectivity of TiO_2 suspensions were made by spectrophotometry. At the same time, the absolute reflectivity of TiO_2 anatase, major component of the

Degussa P-25, can be obtained by tables providing the real and complex parts of the dielectric constant [38] and by applying the Kramers–Kronig relationships, e.g. [39] or other estimations [40]. By combining all these aspects in the wavelength range studied, it was obtained that the reflectivity of the suspensions is around 1%, and it can be neglected. These results agree with those reported by other authors [5].

The other contributions to the total extinction coefficient have also been estimated by spectrophotometric measurements. When a 1 cm width cuvette is placed in the spectrophotometer and far enough from the photodetector (see Fig. 2), the measured transmittance is due to the light that has not been absorbed nor scattered. The extinction coefficient measured in these conditions, by using Eq. (28), includes all the terms appearing in Eq. (29).

On the contrary, when the cuvette was placed near to the photodetector, the transmittance measured was the sum of the contributions of the light transmitted without interacting particles and the light forward scattered. Thus, Q_{fs} can be estimated from the transmittance measurements and by considering the probability that a photon was forward scattered. To evaluate this, let us firstly consider the probability (f_1) that a photon impacts only once against a particle, which will be given by

$$f_1 = n_c P_x (1 - P_x)^{n_c - 1} \tag{30}$$

The probability (f_1') that a photon impacts against a particle and continues with its forwards fly is

$$f_1' = f_1 \left(\frac{Q_{fs}}{Q_e} \right) \tag{31}$$

Q_{fs}/Q_e being the probability that a photon impacting against a particle is forward scattered.

The probability (f_2) that a photon impacts twice against a particle (if particles do not absorb it), is

$$f_2 = \binom{n_c}{2} P_x^2 (1 - P_x)^{n_c - 2} \tag{32}$$

and the probability that, in both impacts, light is forward scattered is $(Q_{fs}/Q_e)^2$.

Then, the percentage of contribution to the transmittance (f_2') of the photons that impact twice against the particles, is

$$f_2' = f_2 \left(\frac{Q_{fs}}{Q_e} \right)^2 \tag{33}$$

Extrapolating for "i" impacts the contribution f_i' to the transmittance is

$$f_i' = \binom{n_c}{i} P_x^i (1 - P_x)^{n_c - i} \left(\frac{Q_{fs}}{Q_e} \right)^i \tag{34}$$

Summarizing, the measured transmittance (T) should take into account all the contributions:

$$T = \sum_{i=0}^{n_c} \binom{n_c}{i} P_x^i (1 - P_x)^{n_c - i} \left(\frac{Q_{fs}}{Q_e} \right)^i \tag{35}$$

Q_{fs} can be estimated by using Eq. (35) since all other terms are known. As the concentrations used were quite low and the diameters were high enough, it has been observed that the sum can be truncated on its fifth term producing less than 1% of error.

Known Q_{fs}, Q_a can be calculated by using Eq. (29), where Q_e is also known and Q_{bs} can be neglected, as explained before. The obtained results for Q_e and Q_{bs} show the same trends observed for σ_a and σ_{fs} (see Fig. 8).

Finally, the values of Q_a and Q_e, together with β and D values previously calculated (Eqs. (16) and (17)), can be used in Eq. (27) to estimate the real kinetic constant k_a, knowing the extensive reaction rate (R) obtained from experimental data. As in the case of the exponential model, k is calculated from k_a by using Eq. (10). Fig. 9 represents the results obtained for k. As made for the exponential model, the quotient between k and the maximum value (k_{max}) is shown as a function of catalyst concentrations tested for each pollutant. By comparison of Figs. 6 and 9, it can be seen that the proposed model (Eq. (27)) follows the trend observed for the experimental data.

4. Conclusions

Models relating the reaction rate of photocatalytic processes to catalyst concentration and radiation absorption have been proposed. The system is divided into cells, with only one catalyst agglomerate in each cell. The extensive reaction rate is the sum of the reaction rates in each cell. The obtained equation is a function of reactants concentration, characteristics and concentration of catalyst, and absorbed radiation. For the estimation of the absorbed radiation, two models are proposed for light propagation through

the reaction medium (exponential and probabilistic model). In both cases, the radiation absorption depends on a parameter β changing according to the position considered. The final expressions provide a relationship between reaction rate, catalyst concentration and radiation absorption. In both cases (exponential and probabilistic model), the predicted trends for the variation of the reaction rate with the catalyst concentration are the same as the ones observed in the photocatalytic treatment of Cr(VI) and phenol. Thus, it can be said that the developed models can explain the behavior of the photocatalytic processes from the kinetic and radiation point of view.

Acknowledgements

Authors are grateful to "Comisión Interministerial de Ciencia y Tecnología, CICYT" (projects AMB98-0357, AMB99-0442 and PPQ2001-3046) for funds received to carry out this work.

References

[1] M.A. Aguado, J. Giménez, S. Cervera-March, Chem. Eng. Commun. 104 (1991) 71.
[2] M.A. Aguado, S. Cervera-March, J. Giménez, J. Chem. Eng. Sci. 50 (1995) 1561.
[3] J. Giménez, M.A. Aguado, S. Cervera-March, J. Mol. Catal. A 105 (1996) 67.
[4] J. Giménez, D. Curcó, M.A. Queral, Catal. Today 54 (1999) 229.
[5] V. Augugliaro, L. Palmisano, M. Schiavello, AIChE J. 37 (1991) 1096.
[6] M. Schiavello, V. Augugliaro, V. Loddo, M.J. Lopez-Munoz, L. Palmisano, Res. Chem. Intermed. 25 (1999) 213.
[7] L. Sun, J.R. Bolton, J. Phys Chem. 100 (1996) 4127.
[8] P.L. Yue, Modelling, scale-up and design of multiphasic photoreactors, in: D.F. Ollis, H. Al-Ekabi (Eds.), Photocatalytic Purification and Treatment of Water and Air, Elsevier, Amsterdam, 1993, p. 495.
[9] O.M. Alfano, R.L. Romero, A.E. Cassano, Chem. Eng. Sci. 41 (1986) 1137.
[10] O.M. Alfano, M.I. Cabrera, A.E. Cassano, J. Catal. 172 (1997) 370.
[11] O.M. Alfano, M.I. Cabrera, A.E. Cassano, J. Adv. Oxid. Technol. 3 (1998) 229.
[12] R.J. Brandi, O.M. Alfano, A.E. Cassano, J. Adv. Oxid. Technol. 3 (1998) 213.
[13] R.J. Brandi, O.M. Alfano, A.E. Cassano, Chem. Eng. Sci. 54 (1999) 2817.
[14] M.I. Cabrera, O.M. Alfano, A.E. Cassano, J. Phys. Chem. 100 (1996) 20043.
[15] M.I. Cabrera, A.C. Negro, O.M. Alfano, A.E. Cassano, J. Catal. 172 (1997) 380.
[16] M.I. Cabrera, O.M. Alfano, A.E. Cassano, J. Adv. Oxid. Technol. 3 (1998) 220.
[17] A.E. Cassano, A.E. Martín, R.J. Brandi, O.M. Alfano, Ind. Eng. Chem. Res. 34 (1995) 2155.
[18] R.L. Romero, O.M. Alfano, A.E. Cassano, J. Adv. Oxid. Technol. 4 (1999) 27.
[19] G. Spadoni, E. Bandini, F. Santarelli, Chem. Eng. Sci. 33 (1978) 517.
[20] T. Yokota, Y. Takahata, H. Nanjo, K. Takahashi, J. Chem. Eng. Jpn. 22 (1989) 537.
[21] T. Yokota, Y. Takahata, Y. Ohto, K. Takahashi, J. Chem. Eng. Jpn. 22 (1989) 548.
[22] D.W. Bahnemann, D. Bockelmann, R. Goslich, Solar Energy Mater. 24 (1991) 564.
[23] D. Curcó, S. Malato, J. Blanco, J. Giménez, P. Marco, Solar Energy 56 (1996) 387.
[24] J. Giménez, D. Curcó, P. Marco, Wat. Sci. Technol. 35 (1997) 207.
[25] C. Kormann, D.W. Bahnemann, M.R. Hoffmann, Environ. Sci. Technol. 25 (1991) 494.
[26] M. Memming, Top. Curr. Chem. 143 (1988) 79.
[27] K. Okamoto, Y. Yamamoto, H. Tanaka, A. Itaya, Bull. Chem. Soc. Jpn. 58 (1985) 2023.
[28] D.F. Ollis, Solar-assisted Photocatalysis for Water Purification: Issues, Data, Questions, in Photochemical Conversion and Storage of Solar Energy, Kluwer Academic Publishers, Dordrecht, The Netherlands, 1991, p. 593.
[29] M.W. Peterson, J.A. Turner, A.J. Nozik, J. Phys. Chem. 95 (1991) 221.
[30] D. Curcó, Kinetic and radiation models for photocatalytic processes, Doctoral Thesis, University of Barcelona, Barcelona, Spain, 1994.
[31] D. Curcó, S. Malato, J. Blanco, J. Giménez, Solar Energy Mater. Solar Cells 44 (1996) 199.
[32] S. Esplugas, J. Giménez, S. Contreras, E. Pascual, M. Rodríguez, Wat. Res. 36 (2002) 1034.
[33] A. Sobczynski, J. Giménez, S. Cervera-March, Monatshefte für Chemie 128 (1997) 1109.
[34] J.M. Herrmann, Catal. Today 24 (1995) 157.
[35] A. Mills, R.H. Davies, D. Worsley, Chem. Soc. Rev. 22 (1993) 417.
[36] M.N. Özisik, Radiative Transfer and Interaction with Conduction and Convection, Webel and Peck, New York, 1973, Chapter 2.
[37] P.C. Hiemenz, Principles of Colloid and Surface Chemistry, in: J.J. Lagowsky (Ed.), Undergraduate Chemistry Series, A Series of Textbooks, vol. 4, Marcel Decker, New York, 1952, Chapter 5.
[38] Landolt-Börnstein, in: O. Madelung (Ed.), Numerical Data and Functional Relationships in Science and Technology, New Series, vol. 17, p. 431;
Landolt-Börnstein, in: O. Madellung, M. Schulz, H. Weiss (Eds.), Semiconductors, Subvolume g;

Landolt-Börnstein, in: O.J.B. Goodenoug, A. Hammet, G. Huber, F. Mulliger, M. Leiss, S.K. Ramasesha, H. Werheit (Eds.), Physics of Non-Tetrahedrally Bonded Binary Compounds, vol. III, Springer, Berlin, 1984.

[39] J.I. Pankove, Optical Processes in Semiconductors, Dover, New York, 1971, Chapter 4.

[40] T.M.R. Viseu, B. Almeida, M. Stchakovsky, B. Drevillon, M.I.C. Ferreira, J.B. Sousa, Thin Solid Films 401 (2001) 216.